Full Paper
doi.org/10.1002/chem.202001825

Metal–Organic Frameworks |Hot Paper|

Effect of Larger Pore Size on the Sorption Properties of Isoreticular Metal–Organic Frameworks with High Number of Open Metal Sites

Pascal D. C. Dietzel,*[a] Peter A. Georgiev,*[b] Morten Frøseth,[c] Rune E. Johnsen,[d] Helmer Fjellvåg,[e] and Richard Blom[c]

Abstract: Four isostructural CPO-54-M metal-organic frameworks based on the larger organic linker 1,5-dihydroxynaphthalene-2,6-dicarboxylic acid and divalent cations (M = Mn, Mg, Ni, Co) are shown to be isoreticular to the CPO-27 (MOF-74) materials. Desolvated CPO-54-Mn contains a very high concentration of open metal sites, which has a pronounced effect on the gas adsorption of N_2, H_2, CO_2 and CO. Initial isosteric heats of adsorption are significantly higher than for MOFs without open metal sites and are slightly higher than for CPO-27. The plateau of high heat of adsorption decreases earlier in CPO-54-Mn as a function of loading per mole than in CPO-27-Mn. Cluster and periodic density functional theory based calculations of the adsorbate structures and energetics show that the larger adsorption energy at low loadings, when only open metal sites are occupied, is mainly due to larger contribution of dispersive interactions for the materials with the larger, more electron rich bridging ligand.

Introduction

Coordination polymers with accessible coordination sites (also called open metal sites or coordinatively unsaturated metal centers) are extremely interesting for application in gas adsorption and separation,[1] catalysis,[2] or sensing.[3] The exposed metal cations of these organic-inorganic hybrid materials often exhibit interaction of significant strength with sorbate molecules, which can span the range from physisorption to chemisorption, where actual coordination complexes with the guest molecules are formed.[4] The interaction between cation and sorbate can be highly specific for a given combination of framework structure, metal cation and sorbate molecule. It is therefore desirable to have a wide selection of compounds available, composing a variety of topologies, and based on different elements as cations so that the most suitable material can be selected for a given application. In addition, a high concentration of open metal sites affects the overall properties of the material, which is particularly beneficial for the use of the material in gas storage or separation.

Many coordination polymers with open metal sites are based on a few recurring structural motifs. One example is the paddle wheel unit found in $Cu_3(btc)_2$/HKUST-1[5] and structurally similar compounds, most frequently formed by copper(II) and zinc(II), but also known to occur in molybdenum(II) and chromium(II) compounds. Another example is the trimeric cluster of condensed octahedra which is present in MIL-88, MIL-100, MIL-101 and similar compounds.[6] The M_3O or $M_3(OH)$ cluster in these is adopted by a range of cations like chromium,[6b,c,7] vanadium,[8] iron,[6a,9] nickel,[10] cobalt,[11] scandium,[12] manganese,[13] indium,[13b,14] and gallium.[15] A third type of inorganic cluster with open metal sites is the M_4Cl cluster in the M-BTT compounds.[16] These three motifs are isolated secondary building blocks that are interconnected in the metal-organic framework by the organic linker. In contrast, another recurring motif is that of an extended one-dimensional chain of condensed metal-oxygen coordination octahedra found in the CPO-27 type compounds (alternatively known as MOF-74,

[a] Prof. Dr. P. D. C. Dietzel
Department of Chemistry, University of Bergen
P.O.box 7803, 5020 Bergen (Norway)
E-mail: Pascal.Dietzel@uib.no

[b] Dr. P. A. Georgiev
Department of Condensed Matter Physics and Microelecetronics
The University of Sofia
J. Bourchier str. 5, 1164 Sofia (Bulgaria)
E-mail: pageorgiev@phys.uni-sofia.bg

[c] Dr. M. Frøseth, Dr. R. Blom
SINTEF Industry
P.O.box 124 Blindern, 0314 Oslo (Norway)

[d] Dr. R. E. Johnsen
Department of Energy Conversion and Storage
Technical University of Denmark
Fysikvej, 2800 Kgs. Lyngby (Denmark)

[e] Prof. H. Fjellvåg
Department of Chemistry, University of Oslo
P.O.box 1033 Blindern, 0313 Oslo (Norway)

Supporting information and the ORCID identification number(s) for the author(s) of this article can be found under: https://doi.org/10.1002/chem.202001825.

© 2020 The Authors. Published by Wiley-VCH GmbH. This is an open access article under the terms of Creative Commons Attribution NonCommercial License, which permits use, distribution and reproduction in any medium, provided the original work is properly cited and is not used for commercial purposes.

© 2020 The Authors. Published by Wiley-VCH GmbH

M_2(dhtp), or M_2(dobdc), where H_4dhtp/H_4dobdc is 2,5-dihydroxyterephthalic acid) which are interconnected by the organic linker to form a honeycomb-like structure. Compounds with this structure can be obtained with several divalent cations like zinc,[17] cobalt,[18] nickel,[19] magnesium,[20] manganese,[21] iron,[22] copper,[23] and cadmium[24] allowing for the exploitation of specific chemical properties of the individual metal cation within a series of isostructural compounds. The condensed nature of the inorganic part of the structure and the highly symmetric crystal structure results in a high number of open metal sites per volume in the structurally stable desolvated materials, which is to date unprecedented among coordination polymers. Consequently, the adsorption properties of the M_2(dhtp) series have been extensively studied[20a,21,23b,25] and are of considerable interest in a number of applications.[26]

The isoreticular approach is a powerful concept for the synthesis of coordination polymers with identical topology and variable pore sizes using organic linking molecules of similar connectivity.[6d,9b,14d,27] The decisive structure-directing factor in the formation of CPO-27/MOF-74 is the way the organic linker interacts with the divalent metal cations in creating the coordination environment of the cation. It is determined by the interplay between the steric arrangement of the α-oxidocarboxylate functional groups of the linker and the ionic radius of the cation. Each α-oxidocarboxylate coordinates four metal cations utilizing a number of coordination modes, including a chelating mode, which imposes restraints on the permissible size of the ions fitting into the structure. In effect, five of six oxygen atoms surrounding each metal cation belong to organic ligand molecules, while the sixth coordinated oxygen atom belongs to a solvent molecule (usually DMF or water). The inorganic secondary building unit of chiral helical chains of metal oxygen coordination octahedra condensed through edges in *cis*-position is a result of the concerted effect of the coordination chemistry of the linker molecules coordinating the metal cations. Alternative organic linkers to 2,5-dihydroxyterephthalic acid also having α-hydroxycarboxylic acid functional groups can be used to obtain isoreticular MOF-74 compounds.[28]

Herein, we report the successful synthesis of a series of coordination polymers, denominated as CPO-54-M (CPO: Coordination Polymer of Oslo), based on divalent cations of manganese, magnesium, cobalt, and nickel and the organic linker 1,5-dihydroxynaphthalene-2,6-dicarboxylic acid (H_4dondc).[28a,b,29] The manganese member of the series has been further characterized. Structure determination of the as-synthesized and desolvated compound confirms the presence of an open metal site in the desolvated compound. The properties of this large pore analogue are compared with the corresponding CPO-27 material using thermal analysis, gas adsorption measurements and computational methods.

Results and Discussion

Synthesis and crystal structure

The CPO-54 compounds were obtained as fine crystalline powders by solvothermal reaction of metal acetate with H_4dondc in a *N*-methyl-2-pyrrolidone (NMP)/water mixture. The powder X-ray diffraction patterns look remarkably similar to the patterns of the CPO-27 series, with a noticeable shift of reflections of corresponding Miller indices towards larger *d* values, indicating an increase in the corresponding lattice parameters (Figure 1 and Table 1). Details of synthesis, powder X-ray diffraction, indexing and profile fits for the four compounds are included in the Supporting Information.

To confirm that CPO-54 is isoreticular with CPO-27, we performed a crystal structure determination of one member of the series, CPO-54-Mn. Because single crystals of a suitable size for crystal structure determination were unavailable, the crystal structure was determined from powder X-ray diffraction data collected at the Swiss-Norwegian Beamlines at the ESRF using simulated annealing and Rietveld refinement techniques implemented in TOPAS (Table 2, full details are given in the Supporting Information).

CPO-54-Mn is indeed isostructural to the CPO-27 compounds. The framework structure resembles a honeycomb (Figure 2) with chains of edge-condensed metal oxygen octahedra located at the corners of the hexagons forming the honeycomb pattern. The metal cations at the center of the octahedra form a threefold helix along the *c* axis. Nearest neighbor helices are of opposite handedness as a consequence of the presence of the inversion center of the centrosymmetric space group. The condensed aromatic rings of the naphthalene derived ligand are stacked in a laminar arrangement along the *c* axis, forming the walls of the honeycomb. The large channel is

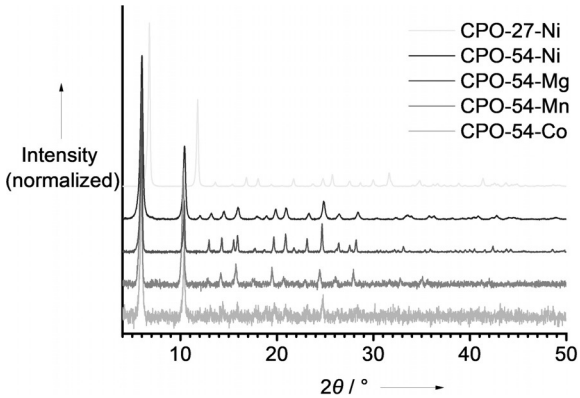

Figure 1. Powder X-ray diffraction patterns of the isostructural CPO-54-M series in comparison to CPO-27-Ni ($\lambda = 1.5406$ Å).

Table 1. Lattice parameters of the CPO-54 compounds as obtained from profile fits of the home lab powder X-ray data (included in the Supporting Information).

Compound	Space group	*a* [Å]	*c* [Å]	*V* [Å^3]
CPO-27-Ni[a]	$R\bar{3}$	25.9783(7)	6.6883(2)	3909.0(2)
CPO-54-Ni[b]	$R\bar{3}$	29.340(6)	6.941 (2)	5175(3)
CPO-54-Mg[b]	$R\bar{3}$	29.408(2)	7.0801(6)	5302.8(7)
CPO-54-Mn[b]	$R\bar{3}$	29.72(2)	7.121(3)	5449(6)
CPO-54-Co[b]	$R\bar{3}$	29.49(2)	6.996(6)	5268(8)

[a] ref. [19]. [b] This work.

© 2020 The Authors. Published by Wiley-VCH GmbH

Table 2. Crystallographic data obtained from the Rietveld refinement of as-synthesized and desolvated CPO-54-Mn.

Compound	CPO-54-Mn (as-synthesized)	CPO-54-Mn (desolvated)
formula	$C_6H_2MnO_3{\cdot}(H_2O)_x$	$C_6H_2MnO_3$
space group (nr)	$R\bar{3}$ (148)	$R\bar{3}$ (148)
Z	18	18
a [Å]	29.7247(12)	29.5185(28)
b [Å]	29.7247(12)	29.5185(28)
c [Å]	7.1376(3)	6.9655(10)
β [°]	120	120
V [Å^3]	5461.6(5)	5256.2(12)
λ [Å]	0.50006	0.50199
2θ range	1.65–25.0	1.5–25.0
R_p	5.34	3.90
R_{wp}	7.08	4.98
R_{exp}	4.69	2.18
Gof	1.51	2.29
R_{Bragg}	2.64	1.76

filled with solvent molecules which were assumed to be predominantly water in the structure refinement. However, some calculated short interatomic distances indicate that there either is significant disorder in the solvent area or it still contains some NMP, as is also indicated by the thermogravimetric analysis (see below). The asymmetric unit contains one metal atom and half a molecule of the organic linker, in agreement with the composition M_2(dondc)·solvent. The hydroxyl and carboxylic acid functional groups of the organic linker are deprotonated, resulting in charge neutrality of the framework. The oxygen atoms of the resultant oxido and carboxylate groups account for five of the six oxygen atoms coordinating the metal cation, while the final atom of the coordination octahedron is part of a solvent molecule.

Thermal analysis and variable-temperature powder X-ray diffraction

Thermal analysis of CPO-54-Mn shows a relatively continuous mass decrease until the material is decomposed (Figure 3 a). There is no apparent plateau that would indicate a temperature range where the desolvated compound is stable. This contrasts with the behavior of the CPO-27 compounds, which show a plateau of stability after removal of the solvent from the pores. However, in light of the structural similarity with the stable CPO-27 frameworks, we found it unlikely that the CPO-54-Mn framework disintegrates because of solvent removal. In fact, the complementary analysis by variable temperature powder X-ray diffraction shows that CPO-54-Mn remains well crystalline until approximately 175–200 °C, indicating that the framework is stable at temperatures usually employed in the pre-treatment of porous coordination polymers before adsorption experiments (Figure 3 b). Above this temperature, the diffraction intensities start to decrease until all crystalline contribution to the pattern has disappeared at around 250–300 °C. Based on these observations, we attribute the lack of a plateau in the TG measurement to the presence of NMP in the pores of the material.

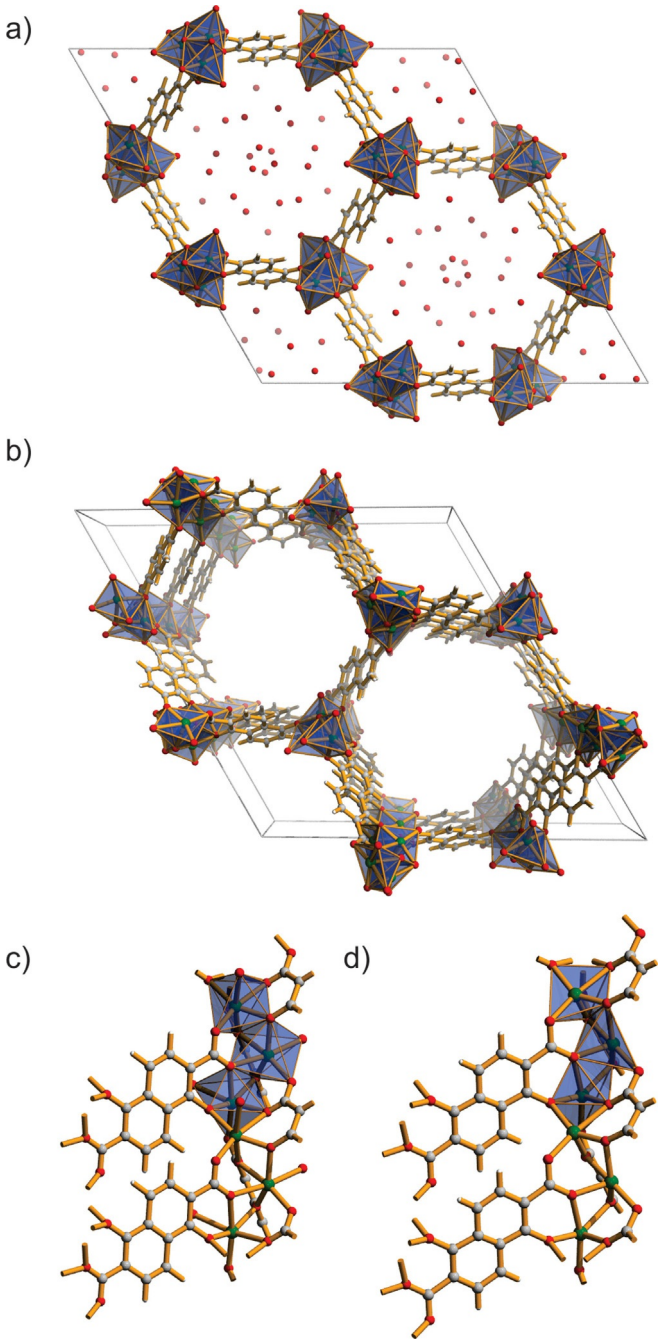

Figure 2. Crystal structure of solvated CPO-54-Mn (a and c) and desolvated CPO-54-Mn (b and d). Cut-out view of the helical chains of condensed metal-oxygen coordination polyhedra (b and d).

Due to the boiling point of NMP of 202 °C, it is unlikely to be removed completely before the framework starts to decompose, that is, solvent removal and combustion of the framework overlap in the thermogravimetric experiment. This interpretation of incomplete solvent removal from the as-synthesized compound is further confirmed by the observation that the lattice parameters never reach the values of the desolvated structure, as obtained for a methanol-washed material.

© 2020 The Authors. Published by Wiley-VCH GmbH

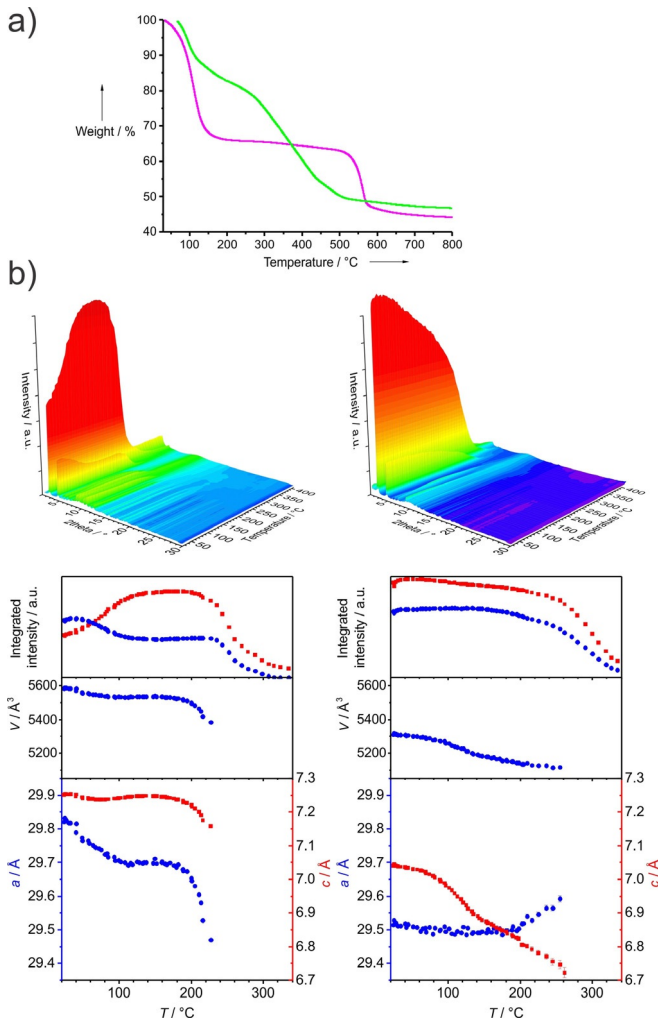

Figure 3. a) Thermogravimetric data of CPO-54-Mn (green) and CPO-27-Mn (magenta). b) variable-temperature powder X-ray diffraction patterns measured using synchrotron radiation for as-synthesized CPO-54-Mn (left, $\lambda = 0.70819$ Å) and CPO-54-Mn washed with methanol (right, $\lambda = 0.7207$ Å). Bottom: Evolution of lattice parameters and integrated intensities of the $(2\bar{1}0)$ and (030) reflections of the two samples.

Crystal structure of empty CPO-54-Mn

As a consequence of the factual thermal stability of the framework, replacement of the high boiling solvent in the pores by lower boiling solvents should make it possible to obtain the desolvated compound with full preservation of the crystalline framework. To demonstrate this, we submersed a sample of CPO-54-Mn in methanol after recovery from synthesis. The supernatant solvent was replaced with fresh methanol once per day for three days. Subsequently, the sample was filtered under inert conditions and the solvent contained in the pores was removed in a dynamic vacuum at 110 °C. Framework stability and absence of solvent from the pore space are confirmed by crystal structure determination of the desolvated compound (Table 2). The coordinated solvent molecule at the metal cation has been removed as well, leaving it in square-pyramidal coordination with the available sixth coordination site accessible from the pore volume (Figure 2b and d). The empty pore volume accounts for 58% of the total volume of the crystal structure. Calculation using the approximation of a perfectly cylindrical shape of the channel along the *c* axis yields an average pore diameter of 13.6 Å (and correspondingly an apparent pore diameter of 10 Å when corrected for the kinetic diameter of a nitrogen probe molecule), compared to 12.3 Å (and an apparent diameter of 8.7 Å) for CPO-27-Mn.

The fact that the framework structure remains stable when the solvent molecule coordinated to the metal cation is removed leads to the creation of an open metal site, which imparts the exceptional adsorption properties onto the CPO-27 (and analogous) compounds. The CPO-27 materials have a record number of open metal sites, for example, 6.58×10^{-3} mol g^{-1} in CPO-27-Mn. CPO-54-Mn has slightly smaller values because of the extended and heavier ligand, with 5.65×10^{-3} mol g^{-1}. Still, it significantly exceeds the values for other MOFs with open metal sites (e.g. HKUST-1/$Cu_3(btc)_2$: 4.55×10^{-3} mol g^{-1}). Our further characterization of CPO-54-Mn had the aim of investigating the effect of the larger ligand and pore size on the properties in comparison to the smaller CPO-27 analogue.

Gas adsorption

Gas adsorption confirms the permanent porosity of the material (Figure 4). The experimental pore volume of 0.58 cm^3 g^{-1} corresponds very well with the value of 0.57 cm^3 g^{-1} calculated from the crystal structure data of the empty framework struc-

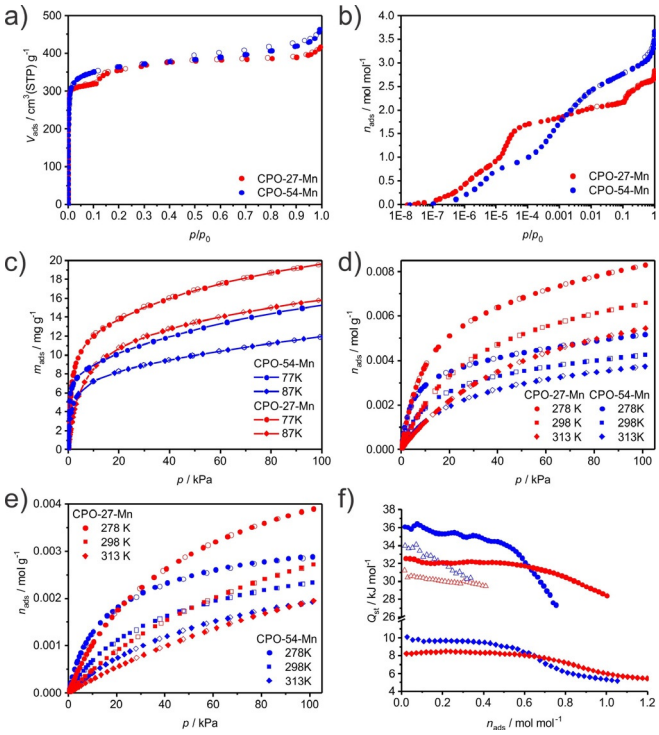

Figure 4. a–b) Nitrogen sorption isotherms at 77 K, c) hydrogen sorption at 77 and 87 K, d) CO_2 sorption at 278, 298 and 313 K, e) CO sorption at 278, 298 and 313 K in CPO-54-Mn (blue) and CPO-27-Mn (red), f) isosteric heat of adsorption in CPO-54-Mn (blue) and CPO-27-Mn (red) for H_2 (diamonds), CO_2 (circles) and CO (triangles) as a function of loading (formula unit).

© 2020 The Authors. Published by Wiley-VCH GmbH

ture. The BET and Langmuir surface areas are 1386 and 1494 $m^2 g^{-1}$, respectively. The good fit between the experimental pore volume obtained from the gas adsorption experiment and the calculated pore volume derived from the crystal structure indicates that the material was indeed successfully and completely desolvated. Furthermore, the semi logarithmic plot shows that nitrogen is adsorbed in a multi-step mechanism that is similar to CPO-27.[30] The first step in the isotherm accounts for adsorption at the thermodynamically most favored adsorption site in the framework, which was identified as the empty coordination site in the vicinity of the M^{II} centers in previous studies on CPO-27.

The volumetric concentration of open metal sites in CPO-54-Mn (3.4 sites per nm^3) is naturally smaller than in the CPO-27-M materials (4.3–4.6 sites per nm^3) because of the larger unit cell of the CPO-54 compound. However, the concentration of open metal sites is still significantly larger than for most other coordination polymers with open metal sites, for example, HKUST-1 (2.6 sites per nm^3), Mn-BTT (1.8 sites per nm^3), or MIL-100 (1.7 sites per nm^3). Open metal sites have a major impact on the adsorption properties of the porous material, which we demonstrate for the adsorption of CO_2, H_2, and CO in CPO-54-Mn (Figure 4). At atmospheric gas pressures, CPO-54-Mn adsorbs 1.5 wt% (7.6 mmol g^{-1}) hydrogen at 77 K, 15.8 wt% (4.3 mmol g^{-1}) CO_2 at 298 K, and 5.1 wt% (1.9 mmol g^{-1}) CO at 298 K. More enlightening for an evaluation of the adsorption properties are the isosteric heats of adsorption, Q_{st}, derived from several measurements at different temperatures. An initial plateau of close to constant heat of adsorption is observed for CO_2 and H_2 before it significantly decreases at loadings larger than approximately 0.5 adsorbate molecules per formula unit (f.u.). The initial heat of adsorption of hydrogen in CPO-54-Mn is relatively unchanged in the range 9–10 kJ mol^{-1} before dropping to 5–6 kJ mol^{-1}. The latter is a typical value for microporous coordination polymers without coordinatively unsaturated metal centers, where the adsorption sites are located near the polar coordinative bond between cation and oxygen or nitrogen from the ligand or at the organic linkers. Such sites are found as secondary and tertiary sites in CPO-27 and other MOFs with open metal sites. The relatively high initial Q_{st} value in CPO-54-Mn reflects the presence of the open metal site. For CO_2, the initial plateau of Q_{st} is in the 34–36 kJ mol^{-1} range before dropping to below 30 kJ mol^{-1} at $n_{ads} > 0.5$ mol f.u.$^{-1}$. The stationary value of the second plateau is not reached at the maximum uptakes observed for the selected temperatures. CO has an initial Q_{st} of 34 kJ mol^{-1} which decreases approximately linearly with increasing loading, reaching 30 kJ mol^{-1} at $n_{ads} = 0.3$ mol f.u.$^{-1}$ which is the maximum uptake at ambient temperature for the maximum pressure attained in our study.

The host–guest structures of various adsorptives in the smaller pore CPO-27 materials have been intensively investigated.[23b,25m,31] The adsorption results for CPO-54 can be interpreted in analogous sense in that the open metal site in the desolvated CPO-54-Mn is the primary adsorption site and therefore represents the major contribution to the high initial isosteric heat of adsorption. It continues to dominate Q_{st} at the successive loadings, where Q_{st} fluctuates only by small amounts. Subsequently, after surpassing the threshold of about 0.5 molecules adsorbate per open metal site and as additional adsorption sites become occupied, the heat of adsorption decreases to lower values typical for coordination polymers without open metal sites.

Similar plateaus of high isosteric heat of adsorption have been observed for guest molecules adsorbed in the CPO-27 materials, in which case the first plateau is even more pronounced and extends until almost full occupancy of the metal site is reached. Such uniform adsorption properties with as high capacity as possible are desirable for most applications in gas storage or separation. On comparison with CPO-27, there are three major differences noticeable in the adsorption behavior of CPO-54-Mn. 1) The maximum heat of adsorption Q_{st}, attained at low loadings, is, for all studied adsorbents, slightly higher for the larger pore CPO-54-Mn material than for CPO-27. 2) The Q_{st} in the CPO-54 material drops earlier than in CPO-27 with increasing loading for all of the studied adsorbents. It approaches values more typical for the non-metal sites already for loadings below 1 adsorbate molecule per f.u. 3) The Q_{st} curve for CO drops faster and approximately linearly relative to the other adsorbates.

The open metal site in the CPO-27 and CPO-54 compounds is located at the corner of the hexagon forming the honeycomb. It is circumscribed by the surrounding walls, while in the majority of compounds with open metal sites, they are part of an isolated inorganic clusters, in which the adsorption site is exposed to the pore volume on all sides except that of the metal cation. The additional boundaries created by the close proximity of the pore walls in CPO-54 thus may lead to an increased contribution of dispersion interactions to the heat of adsorption. In fact, we observe that the initial heat of adsorption for CPO-54-Mn is slightly higher than for CPO-27-Mn. However, as occupation of adsorbate on the open metal site increases, the effect of the larger ratio of wall area to metal site leads to an earlier decrease in Q_{st} for CPO-54 than observed for CPO-27.

Computational study

We performed series of both periodic and cluster model computational studies to investigate the sorption mechanisms in CPO-54-Mn in greater detail and reveal the cause of the differences in the sorption behaviors in comparison to CPO-27.

In very good agreement to experiment, the computed interactions between all of the studied guests, H_2, CO, and CO_2, and the larger framework of CPO-54-Mn appear stronger than those obtained for CPO-27-Mn (Tables S2–S5 in the Supplementary Information). From the periodic model (Table S2) calculations we conclude that this is due to stronger host-guest dispersive interactions. In all cases, both binding energies and distances between adsorbate molecule and metal center indicate a predominantly physisorptive regime, even though orbital interactions are not totally absent. Direct adsorbate-adsorbate interactions within a unit cell of the CPO-54 structure seem to be relatively small, as the binding energies for 0.5, 1, and 2 CO_2 per Mn center change by only up to one kJ mol^{-1}

© 2020 The Authors. Published by Wiley-VCH GmbH

(Table S4). We should point out that, within the structural set up of the present simulations, a loading of 1 corresponds to an adsorbed molecule at each Mn^{II} ion while that of 0.5 has an adsorbate at every Mn^{II} center along a -$(O)_2$-Mn-$(O)_2$- helical chain, but half of the chains remain empty. This represents a computationally cheap way of computing fractional adsorbate loadings, at increments of 0.5 adsorbate molecules per f.u., by always using the 54/72 atom primitive unit cells of the corresponding desolvated CPO-27/54 structures.

Adsorption of CO at the central position of the 92-atom cluster clearly leads to significant charge redistribution along the -$(O)_2$-Mn-$(O)_2$- helical chain, causing a charge drop at the neighboring Mn-ions from +1.28 to +1.01 while the central binding site charge is changed from +1.27 to +1.49, i.e. there is a net charge drop on the three Mn-ions of nearly 0.2 e^-. When CO_2 is adsorbed at the central Mn^{II} ion, the corresponding net charge drop is 0.49 e^-, which is partly compensated by larger dispersive contribution involving both host-guest and guest-guest interactions. These effects directly affect the behavior of the isosteric heat of adsorption of CO and CO_2 in the material, leading to a quick drop from the maximum values at low loading, when neighboring Mn^{II} centers become occupied even before the capacity of the metal sites is exceeded and a significant part of the guest molecules are adsorbed at secondary and tertiary sites close to ligand oxygen atoms and individual ligand fragments. A similar effect was experimentally observed at a microscopic level via in situ FTIR of adsorbed CO in the isostructural CPO-27-Ni material and was also confirmed by DFT based simulations.[32] This kind of "chain binding saturation" can, in principle, explain the relatively sharp dropping Q_{st} curve of CO that contrasts with the usual plateau of relatively constant values for loadings well below 1 molecule per f.u. observed for most adsorptives in these materials.

The dependence of the computed average binding energy as a function of carbon dioxide loading in the two materials shows clear differences. The larger pore volume allows higher loadings of up to 4CO_2/f.u. in CPO-54-Mn (Figure 5 a), compared to CPO-27-Mn (experimentally observed ≈2.2 CO_2/f.u.). These simulations readily relaxed to the stringent convergence criteria on forces (< 1 meV Å^{-1}). The binding energy in CPO-27-Mn (Figure 5 b) slightly increases for loadings up to 1.5 guest molecule per metal center (f.u.). This is due to long range attractive interactions. In contrast, the binding energy in CPO-54-Mn stays constant up to 1 guest molecule per f.u. and is already dropping for 1.5 CO_2 per f.u.

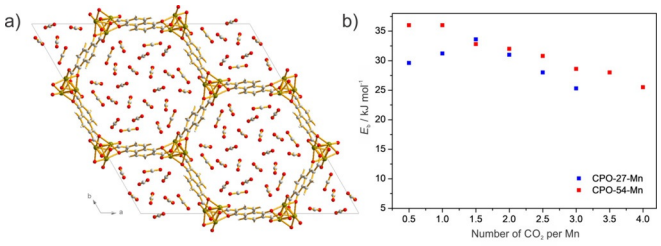

Figure 5. a) Hexagonal unit cell of CPO-54-Mn with 4CO_2/f.u, optimized within the $R\bar{3}$ space group. b) Average binding energy, E_b, of CO_2 in CPO-27-Mn and CPO-54-Mn.

The drop in binding energies, respectively in isosteric heats of adsorption should be compensated at least in part by attractive adsorbate-adsorbate dispersive interactions, which are of larger magnitude for CO_2 than for CO (by about 2 kJ mol^{-1}). Hence, a faster drop in the corresponding Q_{st} is observed for CO, as seen in Figure 4 f. In addition, configurational entropy effects gain significant magnitude compared to the corresponding site binding energies near room temperatures and above. Thus, the corresponding $T\Delta S$ term in the chemical potential, where T is the temperature and ΔS is the change in the corresponding configurational entropy upon adsorption, would rise by about 4.4 kJ mol^{-1} on going from 1/6 metal site occupancy to 6/6 (1 per f.u.) at 298 K. To minimize this effect, the higher the isotherm temperature is, the earlier the molecules start to occupy secondary and possibly also tertiary adsorption sites, gaining configurational entropy which minimizes the free energy at the corresponding loading and temperature conditions, and respectively the gas pressure above the solid by involving adsorption sites of lower binding strengths. As previously shown for the case of H_2, most of the binding energy in CPO-27-Mn and -Cu is due to dispersive interactions.[23b] Similar binding mechanisms operate in CPO-54-Mn (ca. 2/3 of the total binding energy is due to dispersive forces) as seen in the data presented in Table S2. Both periodic and cluster calculations result in a relatively weak red shift of the intramolecular vibrational frequency of the H_2 molecule, comparable to that observed previously in the CPO-27-M materials, and also other MOF structures such as HKUST-1.[25b,32–33] The vibrational frequencies of H_2 at a loading of 18 H_2 molecules per f.u., meaning three sites are fully occupied, are 1) 4165 cm^{-1}, compared to 4178 cm^{-1} for 1 H_2 per f.u, 2) 4240 cm^{-1}, and 3) 4245 cm^{-1} still redshifted by about 70 cm^{-1} as compared to the free state. The corresponding average of the binding energy for H_2 (over the three sets of adsorption sites) drops to 10.8 kJ mol^{-1}, of which a substantial fraction of 8.5 kJ mol^{-1} is due to dispersive interactions (Table S2 in the Supplementary Information).

Similar results have been reported for Mg_2(dobpdc), which has an even larger pore diameter than CPO-54.[34] The isosteric heat of adsorption for CO in CPO-54-Mn shows a more rapid decrease as a function of coverage than with CO_2 and H_2 as adsorptive. Our computational results show that adsorption on a Mn^{II} site leads to a significant decrease of the charge at adjacent metal cations (see Supporting Information). As a consequence, subsequent adsorbate molecules will encounter diminished interaction, which is reflected in the more rapid decrease in Q_{st}.

The part of the pore surface that belongs to the organic linker rather than to the open metal site is larger in CPO-54 than in CPO-27, resulting in a larger number of potential adsorption sites elsewhere than at the metal site, for example, closer to the organic linker, and these are therefore playing a non-negligible role in the trend observed for the isosteric heat of adsorption in CPO-27 and CPO-54. This increased ratio may be responsible for the observation that the first plateau of Q_{st} ends at lower relative loadings in CPO-54 than in CPO-27. This places CPO-54-Mn as intermediate in behavior between CPO-

© 2020 The Authors. Published by Wiley-VCH GmbH

27 and coordination polymers with open metal sites on isolated inorganic clusters.

Conclusions

In summary, we have reported a series of isostructural coordination polymers with honeycomb topology, denominated CPO-54-M with M = Mn, Mg, Ni, and Co. Their crystal structure is isoreticular to that of the CPO-27-M type materials. The CPO-54 materials also contain a high concentration of open metal sites in the desolvated state, which does affect the adsorption properties. We found some intriguing deviations from the observations made on the analogous CPO-27 compounds. 1) Initial Q_{st} values for the CPO-54-Mn material were slightly higher, which is attributed to a larger contribution of dispersive forces originating mainly from the larger organic linker. 2) The Q_{st} curves drop earlier for CPO-54-Mn than for CPO-27-Mn on increased loading to values associated with secondary and tertiary adsorption sites. We attribute this to the more spacious pore of CPO-54-Mn and consequently weaker cooperative adsorbate-adsorbate interactions. This effect is explicitly revealed in the computed binding energies and is, possibly, also due to an anticipated larger entropy effect on the secondary adsorption sites in CPO-54-Mn compared to CPO-27-Mn. 3) A lack of plateau in the Q_{st} curve of CO, (and to a lesser extent for CO_2) is attributed to a "chain saturation affect" due to charge redistribution upon CO adsorption even at very low loadings which reduces the adsorption strengths of metal sites in the close proximity of other metal sites with already adsorbed CO molecules.

The CPO-54 series of compounds is a valuable addition to the field of coordination polymers with open metal sites. It is a derivative of one of the most investigated series of MOFs for separation and/or storage of environmentally and energy relevant adsorptives and size-selective catalysis/synthesis. It has, to the best of our knowledge, the second highest concentration of open metal sites reported for a MOF with a stable rigid structure. We are currently investigating the properties of other members of the series. We expect these investigations to shed light on the interplay between the chemically different open metal sites and their environment in determining the overall adsorption properties of these interesting compounds.

Experimental Section

Crystallographic data: Deposition numbers 1993235 and 1993236 contain the supplementary crystallographic data for this paper. These data are provided free of charge by the joint Cambridge Crystallographic Data Centre and Fachinformationszentrum Karlsruhe Access Structures service.

Acknowledgements

The authors thank the staff at the Swiss–Norwegian Beamlines for their support in performing the experiments at the ESRF. The financial support of the Research Council of Norway through the KOSK (grant 177323) and NANOMAT (grant 182056) programs is gratefully acknowledged. The computational part of this work was supported by the Bulgarian Ministry of Education and Science under the National Research Programme E+: Low Carbon Energy for the Transport and Households, grant agreement D01-214/2018. Access to supercomputing facilities (NESTUM cluster funded by the ERDF Project BG161PO003-1.2.05-0001-C0001) at Sofia Tech Park, Sofia, Bulgaria, is provided by the Faculty of Physics at the University of Sofia, Bulgaria.

Conflict of interest

The authors declare no conflict of interest.

Keywords: adsorption · crystal structure · metal–organic frameworks · molecular modeling · open metal sites

[1] a) C. A. Trickett, A. Helal, B. A. Al-Maythalony, Z. H. Yamani, K. E. Cordova, O. M. Yaghi, *Nat. Rev. Mater.* **2017**, *2*, 17045; b) H. Li, K. Wang, Y. Sun, C. T. Lollar, J. Li, H.-C. Zhou, *Mater. Today* **2018**, *21*, 108–121; c) K. Adil, Y. Belmabkhout, R. S. Pillai, A. Cadiau, P. M. Bhatt, A. H. Assen, G. Maurin, M. Eddaoudi, *Chem. Soc. Rev.* **2017**, *46*, 3402–3430; d) B. Van de Voorde, B. Bueken, J. Denayer, D. De Vos, *Chem. Soc. Rev.* **2014**, *43*, 5766–5788; e) B. Li, H. Wang, B. Chen, *Chem. Asian J.* **2014**, *9*, 1474–1498; f) J. B. DeCoste, G. W. Peterson, *Chem. Rev.* **2014**, *114*, 5695–5727.

[2] a) S. M. J. Rogge, A. Bavykina, J. Hajek, H. Garcia, A. I. Olivos-Suarez, A. Sepulveda-Escribano, A. Vimont, G. Clet, P. Bazin, F. Kapteijn, M. Daturi, E. V. Ramos-Fernandez, F. X. Llabres i Xamena, V. Van Speybroeck, J. Gascon, *Chem. Soc. Rev.* **2017**, *46*, 3134–3184; b) L. Zhu, X.-Q. Liu, H.-L. Jiang, L.-B. Sun, *Chem. Rev.* **2017**, *117*, 8129–8176; c) A. Herbst, C. Janiak, *CrystEngComm* **2017**, *19*, 4092–4117; d) I. Nath, J. Chakraborty, F. Verpoort, *Chem. Soc. Rev.* **2016**, *45*, 4127–4170; e) B. Li, M. Chrzanowski, Y. Zhang, S. Ma, *Coord. Chem. Rev.* **2016**, *307*, 106–129 *Part 2*,; f) M. Zhang, Z.-Y. Gu, M. Bosch, Z. Perry, H.-C. Zhou, *Coord. Chem. Rev.* **2015**, *293–294*, 327–356; g) J. Liu, L. Chen, H. Cui, J. Zhang, L. Zhang, C.-Y. Su, *Chem. Soc. Rev.* **2014**, *43*, 6011–6061.

[3] a) Y. Lv, P. Xu, H. Yu, J. Xu, X. Li, *Sensors and Actuators B: Chemical* **2018**, *262*, 562–569; b) H. Shiozawa, B. C. Bayer, H. Peterlik, J. C. Meyer, W. Lang, T. Pichler, *Sci. Rep.* **2017**, *7*, 2439; c) V. Pentyala, P. Davydovskaya, M. Ade, R. Pohle, G. Urban, *Sensors and Actuators B: Chemical* **2016**, *225*, 363–368; d) I. Stassen, N. Burtch, A. Talin, P. Falcaro, M. Allendorf, R. Ameloot, *Chem. Soc. Rev.* **2017**, *46*, 3185–3241; e) F.-Y. Yi, D. Chen, M.-K. Wu, L. Han, H.-L. Jiang, *ChemPlusChem* **2016**, *81*, 675–690; f) L. V. Meyer, F. Schonfeld, K. Muller-Buschbaum, *Chem. Commun.* **2014**, *50*, 8093–8108.

[4] a) T. L. Easun, F. Moreau, Y. Yan, S. Yang, M. Schroder, *Chem. Soc. Rev.* **2017**, *46*, 239–274; b) E. J. Carrington, I. J. Vitorica-Yrezabal, L. Brammer, *Acta Crystallogr. Sect. B* **2014**, *70*, 404–422.

[5] S. S.-Y. Chui, S. M.-F. Lo, J. P. H. Charmant, A. G. Orpen, I. D. Williams, *Science* **1999**, *283*, 1148–1150.

[6] a) C. Serre, F. Millange, S. Surblé, G. Férey, *Angew. Chem. Int. Ed.* **2004**, *43*, 6285–6289; *Angew. Chem.* **2004**, *116*, 6445–6449; b) G. Férey, C. Serre, C. Mellot-Draznieks, F. Millange, S. Surblé, J. Dutour, I. Margiolaki, *Angew. Chem. Int. Ed.* **2004**, *43*, 6296–6301; *Angew. Chem.* **2004**, *116*, 6456–6461; c) G. Férey, C. Mellot-Draznieks, C. Serre, F. Millange, J. Dutour, S. Surblé, I. Margiolaki, *Science* **2005**, *309*, 2040–2042; d) S. Surblé, C. Serre, C. Mellot-Draznieks, F. Millange, G. Ferey, *Chem. Commun.* **2006**, 284–286.

[7] S. K. Elsaidi, M. H. Mohamed, L. Wojtas, A. J. Cairns, M. Eddaoudi, M. J. Zaworotko, *Chem. Commun.* **2013**, *49*, 8154–8156.

[8] a) K. Barthelet, D. Riou, G. Férey, *Chem. Commun.* **2002**, 1492–1493; b) A. Lieb, H. Leclerc, T. Devic, C. Serre, I. Margiolaki, F. Mahjoubi, J. S. Lee, A. Vimont, M. Daturi, J.-S. Chang, *Microporous Mesoporous Mater.* **2012**, *157*, 18–23.

© 2020 The Authors. Published by Wiley-VCH GmbH

[9] a) M. Dan-Hardi, H. Chevreau, T. Devic, P. Horcajada, G. Maurin, G. Férey, D. Popov, C. Riekel, S. Wuttke, J.-C. Lavalley, A. Vimont, T. Boudewijns, D. de Vos, C. Serre, *Chem. Mater.* **2012**, *24*, 2486 – 2492; b) P. Horcajada, H. Chevreau, D. Heurtaux, F. Benyettou, F. Salles, T. Devic, A. Garcia-Marquez, C. Yu, H. Lavrard, C. L. Dutson, E. Magnier, G. Maurin, E. Elkaïm, C. Serre, *Chem. Commun.* **2014**, *50*, 6872 – 6874; c) L. Peng, M. Asgari, P. Mieville, P. Schouwink, S. Bulut, D. T. Sun, Z. Zhou, P. Pattison, W. van Beek, W. L. Queen, *ACS Appl. Mater. Interfaces* **2017**, *9*, 23957 – 23966; d) A. C. Sudik, A. P. Côté, O. M. Yaghi, *Inorg. Chem.* **2005**, *44*, 2998 – 3000.

[10] a) Y.-S. Wei, K.-J. Chen, P.-Q. Liao, B.-Y. Zhu, R.-B. Lin, H.-L. Zhou, B.-Y. Wang, W. Xue, J.-P. Zhang, X.-M. Chen, *Chem. Sci.* **2013**, *4*, 1539 – 1546; b) J. Jia, X. Lin, C. Wilson, A. J. Blake, N. R. Champness, P. Hubberstey, G. Walker, E. J. Cussen, M. Schröder, *Chem. Commun.* **2007**, 840 – 842; c) S. Ma, J. M. Simmons, D. Yuan, J.-R. Li, W. Weng, D.-J. Liu, H.-C. Zhou, *Chem. Commun.* **2009**, 4049 – 4051; d) G. Ren, S. Liu, F. Wei, F. Ma, Q. Tang, S. Li, *Dalton Trans.* **2012**, *41*, 11562 – 11564.

[11] C. Hua, Q.-Y. Yang, M. J. Zaworotko, *Cryst. Growth Des.* **2017**, *17*, 3475 – 3481.

[12] a) P. D. C. Dietzel, R. Blom, H. Fjellvåg, *Dalton Trans.* **2006**, 2055 – 2057; b) I. A. Ibarra, X. Lin, S. Yang, A. J. Blake, G. S. Walker, S. A. Barnett, D. R. Allan, N. R. Champness, P. Hubberstey, M. Schröder, *Chem. Eur. J.* **2010**, *16*, 13671 – 13679.

[13] a) S. Jeong, X. Song, S. Jeong, M. Oh, X. Liu, D. Kim, D. Moon, M. S. Lah, *Inorg. Chem.* **2011**, *50*, 12133 – 12140; b) J. Jia, F. Sun, T. Borjigin, H. Ren, T. Zhang, Z. Bian, L. Gao, G. Zhu, *Chem. Commun.* **2012**, *48*, 6010 – 6012.

[14] a) X. Gu, Z.-H. Lu, Q. Xu, *Chem. Commun.* **2010**, *46*, 7400 – 7402; b) S.-T. Zheng, J. T. Bu, Y. Li, T. Wu, F. Zuo, P. Feng, X. Bu, *J. Am. Chem. Soc.* **2010**, *132*, 17062 – 17064; c) H. Yang, F. Wang, Y. Kang, T.-H. Li, J. Zhang, *Dalton Trans.* **2012**, *41*, 2873 – 2876; d) X. Zhao, X. Bu, T. Wu, S.-T. Zheng, L. Wang, P. Feng, *Nat. Commun.* **2013**, *4*, 2344; e) Q.-G. Zhai, X. Bu, C. Mao, X. Zhao, P. Feng, *J. Am. Chem. Soc.* **2016**, *138*, 2524 – 2527.

[15] C. Volkringer, T. Loiseau, G. Férey, C. M. Morais, F. Taulelle, V. Montouillout, D. Massiot, *Microporous Mesoporous Mater.* **2007**, *105*, 111 – 117.

[16] a) M. Dincă, A. Dailly, Y. Liu, C. M. Brown, D. A. Neumann, J. R. Long, *J. Am. Chem. Soc.* **2006**, *128*, 16876 – 16883; b) M. Dincă, W. S. Han, Y. Liu, A. Dailly, C. M. Brown, J. R. Long, *Angew. Chem. Int. Ed.* **2007**, *46*, 1419 – 1422; *Angew. Chem.* **2007**, *119*, 1441 – 1444; c) K. Sumida, S. Horike, S. S. Kaye, Z. R. Herm, W. L. Queen, C. M. Brown, F. Grandjean, G. J. Long, A. Dailly, J. R. Long, *Chem. Sci.* **2010**, *1*, 184 – 191; d) M. Asgari, S. Jawahery, E. D. Bloch, M. R. Hudson, R. Flacau, B. Vlaisavljevich, J. R. Long, C. M. Brown, W. L. Queen, *Chem. Sci.* **2018**, *9*, 4579 – 4588.

[17] a) N. L. Rosi, J. Kim, M. Eddaoudi, B. Chen, M. O'Keeffe, O. M. Yaghi, *J. Am. Chem. Soc.* **2005**, *127*, 1504 – 1518; b) P. D. C. Dietzel, R. E. Johnsen, R. Blom, H. Fjellvåg, *Chem. Eur. J.* **2008**, *14*, 2389 – 2397.

[18] P. D. C. Dietzel, Y. Morita, R. Blom, H. Fjellvåg, *Angew. Chem. Int. Ed.* **2005**, *44*, 6354 – 6358; *Angew. Chem.* **2005**, *117*, 6512 – 6516.

[19] P. D. C. Dietzel, B. Panella, M. Hirscher, R. Blom, H. Fjellvåg, *Chem. Commun.* **2006**, 959 – 961.

[20] a) S. R. Caskey, A. G. Wong-Foy, A. J. Matzger, *J. Am. Chem. Soc.* **2008**, *130*, 10870 – 10871; b) P. D. C. Dietzel, R. Blom, H. Fjellvåg, *Eur. J. Inorg. Chem.* **2008**, 3624 – 3632.

[21] W. Zhou, H. Wu, T. Yildirim, *J. Am. Chem. Soc.* **2008**, *130*, 15268 – 15269.

[22] a) E. D. Bloch, L. J. Murray, W. L. Queen, S. Chavan, S. N. Maximoff, J. P. Bigi, R. Krishna, V. K. Peterson, F. Grandjean, G. J. Long, B. Smit, S. Bordiga, C. M. Brown, J. R. Long, *J. Am. Chem. Soc.* **2011**, *133*, 14814 – 14822; b) M. Märcz, R. E. Johnsen, P. D. C. Dietzel, H. Fjellvåg, *Microporous Mesoporous Mater.* **2012**, *157*, 62 – 74.

[23] a) R. Sanz, F. Martinez, G. Orcajo, L. Wojtas, D. Briones, *Dalton Trans.* **2013**, *42*, 2392 – 2398; b) M. H. Rosnes, M. Opitz, M. Frontzek, W. Lohstroh, J. P. Embs, P. A. Georgiev, P. D. C. Dietzel, *J. Mater. Chem. A* **2015**, *3*, 4827 – 4839.

[24] M. Díaz-García, M. Sánchez-Sánchez, *Microporous Mesoporous Mater.* **2014**, *190*, 248 – 254.

[25] a) P. D. C. Dietzel, P. A. Georgiev, J. Eckert, R. Blom, T. Strässle, T. Unruh, *Chem. Commun.* **2010**, *46*, 4962 – 4964; b) S. A. FitzGerald, B. Burkholder, M. Friedman, J. B. Hopkins, C. J. Pierce, J. M. Schloss, B. Thompson, J. L. C. Rowsell, *J. Am. Chem. Soc.* **2011**, *133*, 20310 – 20318; c) T. Pham, K. A. Forrest, R. Banerjee, G. Orcajo, J. Eckert, B. Space, *J. Phys. Chem. C* **2015**, *119*, 1078 – 1090; d) J. Liu, A. I. Benin, A. M. B. Furtado, P. Jakubczak, R. R. Willis, M. D. LeVan, *Langmuir* **2011**, *27*, 11451 – 11456; e) X. Kong, E. Scott, W. Ding, J. A. Mason, J. R. Long, J. A. Reimer, *J. Am. Chem. Soc.* **2012**, *134*, 14341 – 14344; f) L.-C. Lin, J. Kim, X. Kong, E. Scott, T. M. McDonald, J. R. Long, J. A. Reimer, B. Smit, *Angew. Chem. Int. Ed.* **2013**, *52*, 4410 – 4413; *Angew. Chem.* **2013**, *125*, 4506 – 4509; g) D. Yu, A. O. Yazaydin, J. R. Lane, P. D. C. Dietzel, R. Q. Snurr, *Chem. Sci.* **2013**, *4*, 3544 – 3556; h) W. L. Queen, M. R. Hudson, E. D. Bloch, J. A. Mason, M. I. Gonzalez, J. S. Lee, D. Gygi, J. D. Howe, K. Lee, T. A. Darwish, M. James, V. K. Peterson, S. J. Teat, B. Smit, J. B. Neaton, J. R. Long, C. M. Brown, *Chem. Sci.* **2014**, *5*, 4569 – 4581; i) W. D. Wang, B. E. G. Lucier, V. V. Terskikh, W. Wang, Y. Huang, *J. Phys. Chem. Lett.* **2014**, *5*, 3360 – 3365; j) S. A. FitzGerald, J. M. Schloss, C. J. Pierce, B. Thompson, J. L. C. Rowsell, K. Yu, J. R. Schmidt, *J. Phys. Chem. C* **2015**, *119*, 5293 – 5300; k) K. Tan, S. Zuluaga, Q. Gong, Y. Gao, N. Nijem, J. Li, T. Thonhauser, Y. J. Chabal, *Chem. Mater.* **2015**, *27*, 2203 – 2217; l) R. M. Marti, J. D. Howe, C. R. Morelock, M. S. Conradi, K. S. Walton, D. S. Sholl, S. E. Hayes, *J. Phys. Chem. C* **2017**, *121*, 25778 – 25787; m) H. Wu, W. Zhou, T. Yildirim, *J. Am. Chem. Soc.* **2009**, *131*, 4995 – 5000; n) A. Kundu, K. Sillar, J. Sauer, *J. Phys. Chem. Lett.* **2017**, *8*, 2713 – 2718.

[26] a) P. D. C. Dietzel, V. Besikiotis, R. Blom, *J. Mater. Chem.* **2009**, *19*, 7362 – 7370; b) J. Zheng, R. S. Vemuri, L. Estevez, P. K. Koech, T. Varga, D. M. Camaioni, T. A. Blake, B. P. McGrail, R. K. Motkuri, *J. Am. Chem. Soc.* **2017**, *139*, 10601 – 10604; c) S. A. FitzGerald, C. J. Pierce, J. L. C. Rowsell, E. D. Bloch, J. A. Mason, *J. Am. Chem. Soc.* **2013**, *135*, 9458 – 9464; d) H. Oh, I. Savchenko, A. Mavrandonakis, T. Heine, M. Hirscher, *ACS Nano* **2014**, *8*, 761 – 770; e) S. A. Fitzgerald, K. Shinbrough, K. H. Rigdon, J. L. C. Rowsell, M. T. Kapelewski, S. H. Pang, K. V. Lawler, P. M. Forster, *J. Phys. Chem. C* **2018**, *122*, 1995 – 2001; f) D. Britt, H. Furukawa, B. Wang, T. G. Glover, O. M. Yaghi, *Proc. Natl. Acad. Sci. USA* **2009**, *106*, 20637 – 20640; g) E. J. García, J. P. S. Mowat, P. A. Wright, J. Pérez-Pellitero, C. Jallut, G. D. Pirngruber, *J. Phys. Chem. C* **2012**, *116*, 26636 – 26648; h) J. Liu, J. Tian, P. K. Thallapally, B. P. McGrail, *J. Phys. Chem. C* **2012**, *116*, 9575 – 9581; i) T. Remy, S. A. Peter, S. Van der Perre, P. Valvekens, D. E. De Vos, G. V. Baron, J. F. M. Denayer, *J. Phys. Chem. C* **2013**, *117*, 9301 – 9310; j) D.-L. Chen, H. Shang, W. Zhu, R. Krishna, *Chem. Eng. Sci.* **2014**, *117*, 407 – 415; k) S. Dasgupta, S. Divekar, Aarti, A. I. Spjelkavik, T. Didriksen, A. Nanoti, R. Blom, *Chem. Eng. Sci.* **2015**, *137*, 525 – 531; l) X. Hu, S. Brandani, A. I. Benin, R. R. Willis, *Ind. Eng. Chem. Res.* **2015**, *54*, 6772 – 6780; m) D. Bahamon, L. F. Vega, *Chem. Eng. J.* **2016**, *284*, 438 – 447; n) M. Witman, S. Ling, A. Gladysiak, K. C. Stylianou, B. Smit, B. Slater, M. Haranczyk, *J. Phys. Chem. C* **2017**, *121*, 1171 – 1181; o) M. Tagliabue, C. Rizzo, R. Millini, P. D. C. Dietzel, R. Blom, S. Zanardi, *J. Porous Mater.* **2011**, *18*, 289 – 296; p) Y. Peng, V. Krungleviciute, I. Eryazici, J. T. Hupp, O. K. Farha, T. Yildirim, *J. Am. Chem. Soc.* **2013**, *135*, 11887 – 11894; q) P. Mishra, S. Edubilli, B. Mandal, S. Gumma, *J. Phys. Chem. C* **2014**, *118*, 6847 – 6855.

[27] a) A. Schoedel, M. Li, D. Li, M. O'Keeffe, O. M. Yaghi, *Chem. Rev.* **2016**, *116*, 12466 – 12535; b) M. O'Keeffe, O. M. Yaghi, *Chem. Rev.* **2012**, *112*, 675 – 702; c) M. Eddaoudi, J. Kim, N. Rosi, D. Vodak, J. Wachter, M. O'Keeffe, O. M. Yaghi, *Science* **2002**, *295*, 469 – 472; d) M. T. Wharmby, J. P. S. Mowat, S. P. Thompson, P. A. Wright, *J. Am. Chem. Soc.* **2011**, *133*, 1266 – 1269; e) F. Debatin, K. Behrens, J. Weber, I. A. Baburin, A. Thomas, J. Schmidt, I. Senkovska, S. Kaskel, A. Kelling, N. Hedin, Z. Bacsik, S. Leoni, G. Seifert, C. Jäger, C. Günter, U. Schilde, A. Friedrich, H.-J. Holdt, *Chem. Eur. J.* **2012**, *18*, 11630 – 11640; f) V. Guillerm, F. Ragon, M. Dan-Hardi, T. Devic, M. Vishnuvarthan, B. Campo, A. Vimont, G. Clet, Q. Yang, G. Maurin, G. Férey, A. Vittadini, S. Gross, C. Serre, *Angew. Chem. Int. Ed.* **2012**, *51*, 9267 – 9271; *Angew. Chem.* **2012**, *124*, 9401 – 9405; g) N. M. Padial, E. Quartapelle Procopio, C. Montoro, E. López, J. E. Oltra, V. Colombo, A. Maspero, N. Masciocchi, S. Galli, I. Senkovska, S. Kaskel, E. Barea, J. A. R. Navarro, *Angew. Chem. Int. Ed.* **2013**, *52*, 8290 – 8294; *Angew. Chem.* **2013**, *125*, 8448 – 8452; h) G. Barin, V. Krungleviciute, D. A. Gomez-Gualdron, A. A. Sarjeant, R. Q. Snurr, J. T. Hupp, T. Yildirim, O. K. Farha, *Chem. Mater.* **2014**, *26*, 1912 – 1917; i) S. Jeong, D. Kim, S. Shin, D. Moon, S. J. Cho, M. S. Lah, *Chem. Mater.* **2014**, *26*, 1711 – 1719; j) H. Chun, D. N. Dybtsev, H. Kim, K. Kim, *Chem. Eur. J.* **2005**, *11*, 3521 – 3529; k) S. Yang, X. Lin, A. Dailly, A. J. Blake, P. Hubberstey, N. R. Champness, M. Schröder, *Chem. Eur. J.* **2009**, *15*, 4829 – 4835; l) H.-M. Wen, B. Li, L. Li, R.-B. Lin, W. Zhou, G. Qian, B. Chen, *Adv. Mater.* **2018**, *30*, 1704792; m) I. Spanopoulos, C. Tsangarakis, E. Klontzas, E. Tylianakis, G. Froudakis, K. Adil, Y. Belmabkhout, M. Eddaoudi, P. N. Trikalitis, *J. Am. Chem. Soc.* **2016**, *138*, 1568 – 1574; n) R. Banerjee, H. Furukawa, D. Britt, C. Knobler, M. O'Keeffe, O. M. Yaghi, *J. Am. Chem. Soc.* **2009**, *131*, 3875 – 3877; o) F. Moreau, D. I. Kolokolov, A. G. Stepanov, T. L. Easun, A. Dailly, W. Lewis,

© 2020 The Authors. Published by Wiley-VCH GmbH

A. J. Blake, H. Nowell, M. J. Lennox, E. Besley, S. Yang, M. Schröder, *Proc. Natl. Acad. Sci. USA* **2017**, *114*, 3056 – 3061; p) T. C. Wang, W. Bury, D. A. Gómez-Gualdrón, N. A. Vermeulen, J. E. Mondloch, P. Deria, K. Zhang, P. Z. Moghadam, A. A. Sarjeant, R. Q. Snurr, J. F. Stoddart, J. T. Hupp, O. K. Farha, *J. Am. Chem. Soc.* **2015**, *137*, 3585 – 3591; q) J. Liu, B. Lukose, O. Shekhah, H. K. Arslan, P. Weidler, H. Gliemann, S. Bräse, S. Grosjean, A. Godt, X. Feng, K. Müllen, I.-B. Magdau, T. Heine, C. Wöll, *Sci. Rep.* **2012**, *2*, 921; r) H. Furukawa, Y. B. Go, N. Ko, Y. K. Park, F. J. Uribe-Romo, J. Kim, M. O'Keeffe, O. M. Yaghi, *Inorg. Chem.* **2011**, *50*, 9147 – 9152; s) D. Zhao, D. J. Timmons, D. Yuan, H.-C. Zhou, *Acc. Chem. Res.* **2011**, *44*, 123 – 133; t) F. Song, C. Wang, J. M. Falkowski, L. Ma, W. Lin, *J. Am. Chem. Soc.* **2010**, *132*, 15390 – 15398; u) L. Ma, J. M. Falkowski, C. Abney, W. Lin, *Nat. Chem.* **2010**, *2*, 838; v) D. Yuan, D. Zhao, D. Sun, H.-C. Zhou, *Angew. Chem. Int. Ed.* **2010**, *49*, 5357 – 5361; *Angew. Chem.* **2010**, *122*, 5485 – 5489; w) X. Lin, J. Jia, X. Zhao, K. M. Thomas, A. J. Blake, G. S. Walker, N. R. Champness, P. Hubberstey, M. Schröder, *Angew. Chem. Int. Ed.* **2006**, *45*, 7358 – 7364; *Angew. Chem.* **2006**, *118*, 7518 – 7524.

[28] a) P. D. C. Dietzel, R. E. Johnsen, M. Frøseth, R. Blom, H. Fjellvåg, in *Abstracts of the 16th International Zeolite Conference Joint with the 7th International Mesostructured Materials Symposium: IZC- IMMS* **2010** (Eds.: C. Colella, P. Aprea, B. de Gennaro, B. Liguoris), Sorrento, Italy, July 4 – 9, 2010 (ISBN: 9788889976296), abstract title: *Isoreticular coordination polymers with honeycomb topology*; b) P. D. C. Dietzel, M. Frøseth, R. Blom, R. E. Johnsen, H. Fjellvåg, *in 2nd International Conference on Metal-Organic Frameworks and Open Framework Compounds*, Marseille, France, **2010**, https://dechema.de/en/mof2010.html; c) T. M. McDonald, W. R. Lee, J. A. Mason, B. M. Wiers, C. S. Hong, J. R. Long, *J. Am. Chem. Soc.* **2012**, *134*, 7056 – 7065; d) H. Deng, S. Grunder, K. E. Cordova, C. Valente, H. Furukawa, M. Hmadeh, F. Gándara, A. C. Whalley, Z. Liu, S. Asahina, H. Kazumori, M. O'Keeffe, O. Terasaki, J. F. Stoddart, O. M. Yaghi, *Science* **2012**, *336*, 1018 – 1023; e) W. Meng, Y. Zeng, Z. Liang, W. Guo, C. Zhi, Y. Wu, R. Zhong, C. Qu, R. Zou, *ChemSusChem* **2018**, *11*, 3751 – 3757; f) H. Montes-Andrés, G. Orcajo, C. Mellot-Draznieks, C. Martos, J. A. Botas, G. Calleja, *J. Phys. Chem. C* **2018**, *122*, 28123 – 28132; g) L. Peng, S. Yang, S. Jawahery, S. M. Moosavi, A. J. Huckaba, M. Asgari, E. Oveisi, M. K. Nazeeruddin, B. Smit, W. L. Queen, *J. Am. Chem. Soc.* **2019**, *141*, 12397 – 12405; h) P. I. Scheurle, A. Mähringer, A. C. Jakowetz, P. Hosseini, A. F. Richter, G. Wittstock, D. D. Medina, T. Bein, *Nanoscale* **2019**, *11*, 20949 – 20955.

[29] J. S. Yeon, W. R. Lee, N. W. Kim, H. Jo, H. Lee, J. H. Song, K. S. Lim, D. W. Kang, J. G. Seo, D. Moon, B. Wiers, C. S. Hong, *J. Mater. Chem. A* **2015**, *3*, 19177 – 19185.

[30] M. H. Rosnes, D. Sheptyakov, A. Franz, M. Frontzek, P. D. C. Dietzel, P. A. Georgiev, *PCCP* **2017**, *19*, 26346 – 26357.

[31] a) P. D. C. Dietzel, R. E. Johnsen, H. Fjellvåg, S. Bordiga, E. Groppo, S. Chavan, R. Blom, *Chem. Commun.* **2008**, 5125 – 5127; b) Y. Liu, H. Kabbour, C. M. Brown, D. A. Neumann, C. C. Ahn, *Langmuir* **2008**, *24*, 4772 – 4777; c) A. C. McKinlay, B. Xiao, D. S. Wragg, P. S. Wheatley, I. L. Megson, R. E. Morris, *J. Am. Chem. Soc.* **2008**, *130*, 10440 – 10444; d) H. Wu, J. M. Simmons, G. Srinivas, W. Zhou, T. Yildirim, *J. Phys. Chem. Lett.* **2010**, *1*, 1946 – 1951; e) S. Xiang, W. Zhou, Z. Zhang, M. A. Green, Y. Liu, B. Chen, *Angew. Chem. Int. Ed.* **2010**, *49*, 4615 – 4618; *Angew. Chem.* **2010**, *122*, 4719 – 4722; f) W. L. Queen, C. M. Brown, D. K. Britt, P. Zajdel, M. R. Hudson, O. M. Yaghi, *J. Phys. Chem. C* **2011**, *115*, 24915 – 24919; g) K. Sumida, C. M. Brown, Z. R. Herm, S. Chavan, S. Bordiga, J. R. Long, *Chem. Commun.* **2011**, *47*, 1157 – 1159; h) W. L. Queen, E. D. Bloch, C. M. Brown, M. R. Hudson, J. A. Mason, L. J. Murray, A. J. Ramirez-Cuesta, V. K. Peterson, J. R. Long, *Dalton Trans.* **2012**, *41*, 4180 – 4187; i) O. V. Magdysyuk, F. Adams, H. P. Liermann, I. Spanopoulos, P. N. Trikalitis, M. Hirscher, R. E. Morris, M. J. Duncan, L. J. McCormick, R. E. Dinnebier, *PCCP* **2014**, *16*, 23908 – 23914; j) J. S. Lee, B. Vlaisavljevich, D. K. Britt, C. M. Brown, M. Haranczyk, J. B. Neaton, B. Smit, J. R. Long, W. L. Queen, *Adv. Mater.* **2015**, *27*, 5785 – 5796; k) M. I. Gonzalez, J. A. Mason, E. D. Bloch, S. J. Teat, K. J. Gagnon, G. Y. Morrison, W. L. Queen, J. R. Long, *Chem. Sci.* **2017**, *8*, 4387 – 4398; l) B. Pato-Doldán, M. H. Rosnes, P. D. C. Dietzel, *ChemSusChem* **2017**, *10*, 1710 – 1719; m) E. D. Bloch, W. L. Queen, R. Krishna, J. M. Zadrozny, C. M. Brown, J. R. Long, *Science* **2012**, *335*, 1606 – 1610; n) C. M. Brown, A. J. Ramirez-Cuesta, J.-H. Her, P. S. Wheatley, R. E. Morris, *Chem. Phys.* **2013**, *427*, 3 – 8.

[32] N. Drenchev, M. Mihaylov, P. D. C. Dietzel, A. Albinati, P. A. Georgiev, K. Hadjiivanov, *J. Phys. Chem. C* **2016**, *120*, 23083 – 23092.

[33] a) N. Drenchev, M. H. Rosnes, P. D. C. Dietzel, A. Albinati, K. Hadjiivanov, P. A. Georgiev, *J. Phys. Chem. C* **2018**, *122*, 17238 – 17249; b) J. G. Vitillo, L. Regli, S. Chavan, G. Ricchiardi, G. Spoto, P. D. C. Dietzel, S. Bordiga, A. Zecchina, *J. Am. Chem. Soc.* **2008**, *130*, 8386 – 8396; c) C. Prestipino, L. Regli, J. G. Vitillo, F. Bonino, A. Damin, C. Lamberti, A. Zecchina, P. L. Solari, K. O. Kongshaug, S. Bordiga, *Chem. Mater.* **2006**, *18*, 1337 – 1346; d) N. Nijem, L. Kong, Y. Zhao, H. Wu, J. Li, D. C. Langreth, Y. J. Chabal, *J. Am. Chem. Soc.* **2011**, *133*, 4782 – 4784.

[34] J. G. Vitillo, G. Ricchiardi, *J. Phys. Chem. C* **2017**, *121*, 22762 – 22772.

Manuscript received: April 15, 2020
Accepted manuscript online: May 19, 2020
Version of record online: September 24, 2020

© 2020 The Authors. Published by Wiley-VCH GmbH